BUCKHOLZ TRAFFIC
3585 KORI ROAD
JACKSONVILLE, FLORIDA 32257
www.buckholztraffic.com
(904) 886-2171 jwbuckholz@aol.com

THE REAL-TIME ESTIMATION OF DELAY AT SIGNALIZED INTERSECTIONS

Jeffrey W. Buckholz, P.E.[1]

ABSTRACT. The efficient operation of signalized intersections is a pertinent topic throughout the world. Providing a real-time evaluation system that allows intersections to be operated at maximum efficiency has the potential for tremendous benefit. An empirical procedure has been developed for estimating intersection delay in real-time given limited information. The procedure, which can be applied under congested traffic conditions as well as free flow conditions, estimates the length of vehicle queues and associated stopped delay. To ensure reasonableness, the results of the empirical delay estimation procedure are theoretically constrained using upper and lower bounds derived from historical peak hour factors. The end result is a theoretically constrained delay estimation procedure that, when fully implemented, can be used for project evaluation, real-time adjustment of signal timings, and intersection capacity analysis.

INTRODUCTION

Since the efficient operation of signalized intersections is a pertinent topic throughout the world, providing a real-time evaluation system that allows such intersections to be operated at maximum efficiency has the potential for tremendous benefit. Reductions in travel time would be the primary benefit, along with associated reductions in fuel usage and vehicle emissions. The benefits would accrue "24/7" in that signalized intersections function around the clock. According to Tarnoff and Ordonez (2004), in the United States alone there are approximately 265,000 signalized intersections and the delays at these signalized intersections contribute an estimated 25% to total highway system delay.

[1] President, JW Buckholz Traffic Engineering Inc and Adjunct Professor, University of North Florida, Jacksonville, Florida, email: jwbuckholz@aol.com

The benefit of corridor re-timing programs, signal phasing changes, and intersection geometric improvements can be properly evaluated only if a realistic assessment of the change in overall vehicular delay is determined. Collecting delay data by hand, as described in Chapter 16, Appendix A of the 2000 Highway Capacity Manual is a labor-intensive task that must, by practical necessity, be limited to brief data collection periods. In addition, it is particularly difficult to collect delay data during over-saturated conditions even though this is exactly when knowledge of delay levels is most critical. Consequently, under congested conditions, delay calculations that are based on manual information can be considered both piecemeal and of dubious accuracy.

A properly automated method for collecting delay data would provide the needed evaluation data for all pertinent periods. Such a system would also provide reasonable estimations of delay, even during over-saturated conditions. Video detection systems, vehicle re-identification systems using inductance loops, and probe monitoring all offer the potential of being able to calculate (or reasonably estimate) vehicular delay in real time. The resulting delay data could then be used for project evaluation or for the real-time modification of controller settings**.**

Unfortunately, the direct measurement of stopped delay via video detection or inductance loops falls prey to a number of practical limitations, ranging from detection inaccuracies to field of view limitations. Accurate estimation of approach delay is of most interest during peak periods when traffic demand is at its greatest. It is during these critical periods that extensive queues typically form; queues that can extend well beyond the field of view of any intersection-based detection system. Consequently, when we most need an accurate estimation of approach delay is exactly when we are least likely to obtain it from conventional detection systems.

Using real-time delay obtained from intersection-based field measurements for project evaluation purposes (such as signal retiming evaluation) also provide an important supplement to traditional before and after travel time runs, which completely ignore the delay experienced by side street motorists or main street left turn motorists. A rather large leap forward in project evaluation and real-time traffic control could be taken if we are able to develop a widely applicable, robust procedure for calculating vehicular delay on the fly.

The literature search concerning this topic revealed that a number of investigators have approached the problem at hand, investigating various techniques designed to improve the estimation of travel time and delay along the through lanes of an arterial corridor. However, the research effort described herein is unique in attempting to estimate delay in a manner that is directly applicable to the minor movements of the intersection as well. In addition, none of the previous research has dealt with the real-world problem of queues that extend beyond the detection system for some period of time; either short-lived queues that occur during under-saturated conditions because of spurts in activity or longer-lived, recurring queues that occur during over-saturated conditions. This appears to be the only research that is attempting to intelligently “estimate that which cannot be easily measured” with respect to intersection delay.

The objectives of the research would best be achieved using actual field data. However, detailed field data is not only expensive and time consuming to collect; one cannot safely or expeditiously manipulate field data in order to experiment at controlled volume levels or cycle lengths. Analyzing substantially over-saturated systems is also very difficult using actual field data as queue lengths can

become quite extensive; spilling over into adjacent signalized intersections**.** Therefore, theoretical research work was carried out in the laboratory using the CORSIM micro-simulation model. CORSIM allows us to quickly simulate a variety of real-world conditions in a relatively realistic manner and to accumulate important measures of effectiveness, including delay.

CORSIM was specifically used to examine how measured delay differs from actual delay when queues exceed the limits of the detection system. In order to investigate such differences, it was necessary to assume a certain "field of view" for the simulation runs. The field of view is defined as the number of vehicles on an intersection approach lane that can be accurately measured by the detection system when the vehicles are queued at the stop bar. A field of view of 12 vehicles was used in most of the examples associated with this theoretical work. This would be a reasonable field of view for a modern video detection system.

A limited field of view produces a situation where arrivals at the back of the queue cannot be observed. This incomplete information makes it impossible to calculate the resulting delay. However, using the methodology contained in this paper, the delay can be reasonably estimated under a rather wide variety of conditions. The procedure that was developed in response to the challenge of estimating non-visible delay begins by calculating an "estimated arrival rate", which is based on the number of vehicles entering the field of view. If the back end of the queue is not visible, the procedure modifies the estimated arrival rate upward using an empirical power function in an attempt to predict the real arrival rate. This power function adjusts the rate in a manner that varies with the amount of time during which the back end of the queue is not visible. Finally, the arrival rate is adjusted once again to account for queue propagation effects.

A major advantage of this approach is that the resulting estimated queues and associated delay are immediately calculated on a second-by-second basis, in real time. A major disadvantage of the approach is that there is no theoretical relationship between the adjusted arrival rate and the real arrival rate. Hence, two different arrival patterns that result in the same number of vehicles entering the field of view during the analysis period can produce similar delay results. This problem is most evident when the length of time that the end of the queue is not visible covers most of the analysis period.

Fortunately, it is possible to calculate a set of theoretical upper and lower bounds on the solution space by using information obtained at the end of the analysis period, when all queues are visible and the arrival rate is known. In order to make any type of reasonable delay estimation, all queues must dissipate prior to the end of the analysis period. Once queues become fully visible, an accurate calculation of the arrival rate can be made. Knowing this arrival/departure rate and knowing the total number of vehicles that have crossed the stop line during the entire hour we can, by assuming a reasonable minimum peak hour factor, work backwards through the period to identify arrival curves that serve as both lower and upper bounds. These theoretical bounds can be used, in an ex post facto manner, to bracket the previously discussed real-time delay estimation procedure.

The theoretical upper and lower bounds on the delay solution take the form of cumulative arrival curves. Vehicular delay is obtained through consideration of the area between these cumulative arrival curves and the associated cumulative departure curve. Within this document it is demonstrated that, contrary to popular belief, the area between the arrival and departure curves is not

the delay incurred by approaching vehicles. An evaluation of trajectory analysis during over-saturated conditions is used to rectify the difference between the true delay and the area between the cumulative arrival and cumulative departure curves.

ANALYSIS

In order to obtain the data needed for analysis, a visual basic program called TSDViewer was developed which reads the output file of CORSIM and produces, on a second-by-second basis, a variety of information pertaining to the number of vehicles crossing various checkpoints and arriving and departing queues. BuckQ, a visual basic application program for Excel was then developed to read the data provided by TSDViewer and to produce a variety of useful information based on this data. BuckQ provides, for a one-hour analysis time frame having four 15-minute periods, a second-by-second tabulation of items such as queue length, back of queue position, stopped delay, move-up delay and control delay. It also provides a host of ancillary capabilities, including automated calculation of: start-up-lost-time, saturation flow, and capacity by cycle; HCM queuing and delay information by 15-minute period; and arrival type by 15-minute period. In addition, BuckQ allows evaluation of arrival patterns using a chi-squared goodness-of-fit test and provides extensive graphing capabilities. However, the most important feature of BuckQ is its ability to accommodate second-by-second queue and delay prediction procedures and its ability to compare the results of these procedures to CORSIM results (with CORSIM serving as the "ground truth"). Using BuckQ, delay prediction algorithms can be tested to see how well they perform and the results presented in a graphical format.

A third visual basic program named DTDiagram was also developed as part of this research. This program reads the CORSIM output file and produces trajectory information (a series of time-distance points) for each vehicle. The data produced by DTDiagram is read by BuckTRAJ, a fourth visual basic program that was developed as part of this research to calculate, for each vehicle, all of the components of control delay. The procedures used by BuckQ addresses delay from an input/output prospective wherein delay is accumulated on a second-by-second basis, information that is not provided by BuckTRAJ. On the other hand, BuckTRAJ provides delay information for individual vehicles, vehicles that cannot be tracked with the input/output approach utilized by BuckQ.

The CORSIM runs made use of a very simple case, the intersection of 2 one-way streets, each having a single approach lane. No trucks were placed into the traffic stream and no turns were allowed. A random (Poisson) arrival pattern was set with arrival rates varying each 15-minutes during a one-hour analysis time frame. The intersection was controlled by a 2-phase semi-actuated traffic signal and delay data was collected and analyzed only for the actuated side street approach.

In order to make use of existing detection systems it becomes necessary to measure that portion of the stopped delay that can be observed and then intelligently estimate what cannot be observed (see Figure 1).

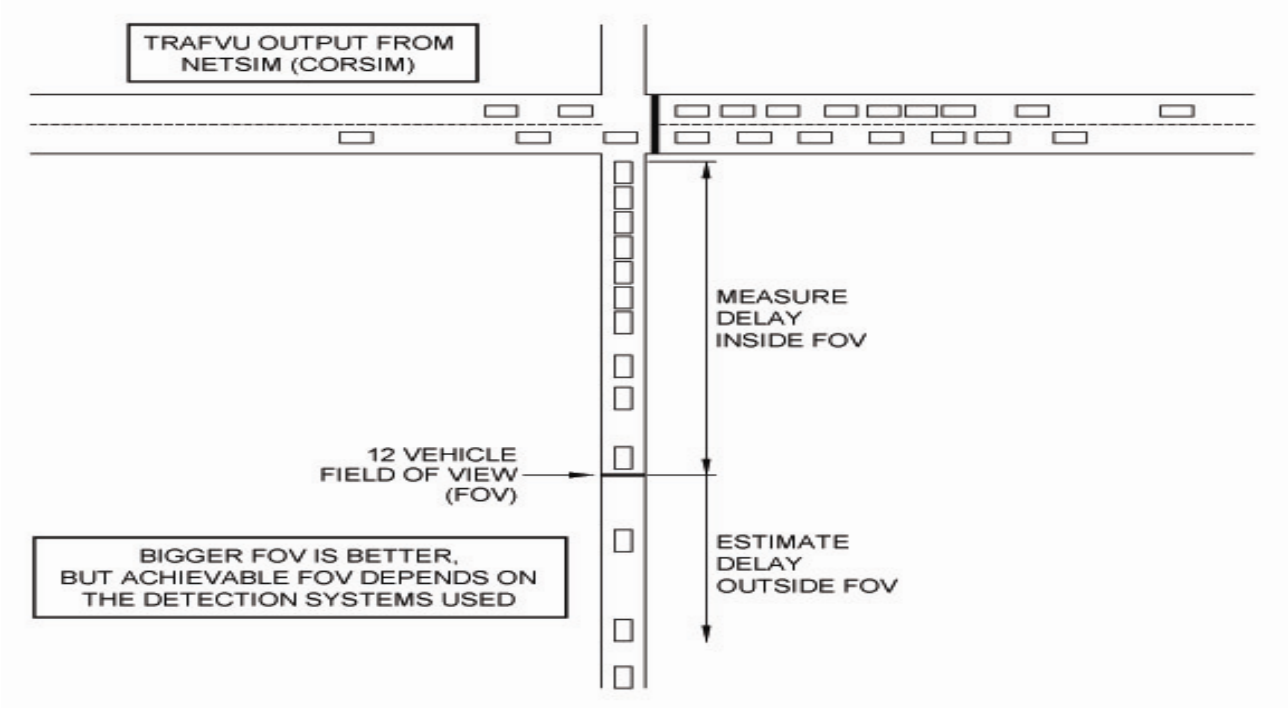

Figure 1. Measured versus estimated delay

The result is the methodology produced by this research, a methodology that measures **visible stopped delay;** stopped delay that occurs within the Field of View (FOV) of the detection system and then uses various analytical techniques to predict **non-visible stopped delay;** stopped delay that occurs outside the FOV. The portion of the queue that is outside the FOV is referred to in this research as the **non-visible queue** (see Figure 2) and the period of time during which non-visible queues are present is referred to as the **blind period**.

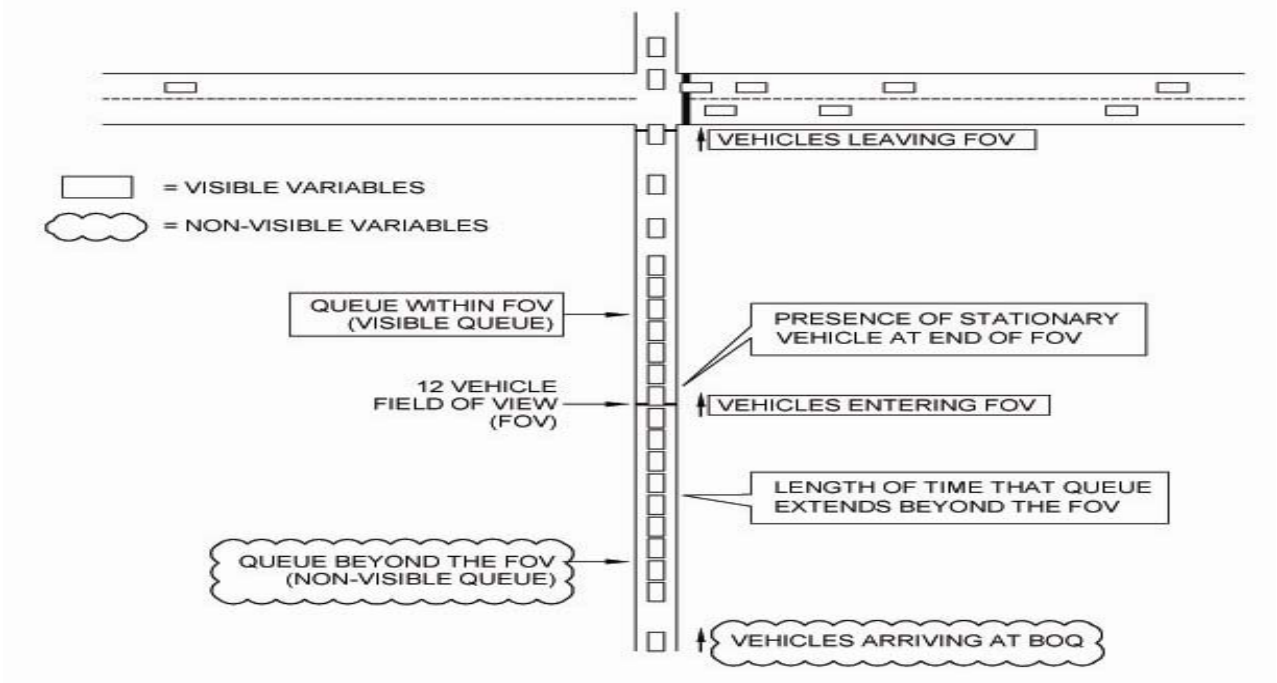

Figure 2. Visible and non-visible variables

When the side street approach under investigation receives the red indication, vehicles begin to queue at the stop bar. The time during which the entire queue is within the FOV and can be "seen" by the detection system is referred to as the **visible period**.

Eventually, the queue fills-up the FOV and the detection system can no longer measure the exact queue length. When this occurs, the system transitions from a visible period into a **blind period** and the prediction process must begin for the non-visible queue. During this blind period, vehicles attach themselves to the end of the non-visible queue at some unknown rate, referred to as the **actual arrival rate**. The portion of the blind period during which vehicles can attach themselves to the back of the non-visible queue, but cannot leave the front of the non-visible queue since the signal has not yet turned green and there are vehicles queued ahead of them, is referred to as the **rising queue blind period**.

Eventually the side street approach receives the green indication and vehicles on that approach begin to cross the stop bar. The visible queue shrinks from the front until the last vehicle in the FOV begins to move and the visible queue becomes zero. At this point, vehicles can begin to depart the non-visible queue from the front while they continue to attach to the back of the non-visible queue at the unknown rate. We refer to this portion of the blind period where vehicles can both attach themselves to the back of the non-visible queue and leave the front of the non-visible queue, as the **falling queue blind period**. The length of the non-visible queue is typically falling during this period since vehicles almost always depart the front of the queue at a much faster rate than they arrive at the back of the queue.

For example, assume a field of view (FOV) of 12 vehicles. When the visible queue extends to a point where the 12^{th} position is filled by a queued vehicle, the rising queue portion of the blind period begins. After some period of time the signal turns green and, eventually, the vehicle in position 12 moves forward. When this vehicle moves forward the rising queue portion of the blind period ends and the falling queue portion of the blind period begins. After some additional period of time, a gap of sufficient duration (such as 5 seconds) is encountered between successive vehicles entering the FOV, signaling that the end of the queue has come into view. When this happens, the blind period has ended.

Many blind periods may exist over a given analysis time frame, with the number of blind periods depending on the number of times that the end of the actual queue goes out of, and then comes back into, the field of view.

If a vehicle does not enter the queue FOV for some sufficiently long period of time (such as 5 seconds), and if another queue does not fill the FOV prior to this 5-second period, then the blind period is considered to have ended and the system returns to a visible state where the actual queue length is known. When this occurs it is assumed that there no longer exists a non-visible queue (i.e., the non-visible queue has been "flushed out"). However, if this 5-second headway does not occur before the FOV is once again filled with queued vehicles, then the system transitions from one blind period into another with no intervening period of visibility. When this happens, **adjacent blind periods** occur. As one might expect, the problem of estimating the length of non-visible queues and their associated delay becomes more difficult (and, hence, more approximate) as the frequency of adjacent blind periods increases. As we shall soon discover, the number of adjacent blind periods is

an important variable when attempting to predict the length of the non-visible queue and its associated stopped delay.

One of the central elements of this research is the development of a predictive algorithm that determines a reasonable value for the stopped delay associated with the non-visible portion of the queue. The first component of the algorithm is an estimation technique that uses the rate of arrivals into the FOV to estimate the arrival rate at the back of the non-visible queue.

Non-Visible Queue <u>Estimation</u> Technique

This technique assumes that vehicles arrive at the back of the queue at a uniform rate during the full extent of the blind period. The arrival rate is calculated using the number of vehicles that enter the FOV during the blind period. For example, if the blind period last for 32 seconds and 8 vehicles enter the FOV, then the estimated arrival rate is 8 vehicles/32 seconds or 0.25 vehicles/second. All of these vehicles enter the FOV during the falling queue portion of the blind period, a time when traffic is freely flowing thru the FOV. Vehicles are also assumed to depart the non-visible queue at a constant rate of 1 vehicle per second during the Falling Queue Blind Period. Since the departure rate is almost always greater than the arrival rate, the non-visible queue shrinks in size and, if sufficient green time is provided, eventually disappears during this period.

Initial experiments have verified that this particular technique does a good job of estimating non-visible queues and delays when a period of visibility follows the blind period. However, when traffic volumes intensify, it is often the case that the FOV fills with queued vehicles without a 5-second headway being observed. In this case, "adjacent blind periods" occur. The problem with adjacent blind periods is twofold: 1) The true number of vehicles that arrived during the blind period is unknown because the FOV fills-up and all of the arrivals do not come into the FOV, and 2) One never really knows where the true end of the queue is, forcing non-visible queue length estimations to be made that depend on previous non-visible queue length estimations. Additional adjustments are needed to handle adjacent blind periods.

Non-Visible Queue <u>Adjustment</u> Technique

The adjacent blind period counter increments by a value of 1 whenever a blind period is followed by another blind period, and resets to zero when a period of visibility occurs. The estimated arrival rate is increased using an additive power function of the following form:

$$AR_{adj} = AR_{est} + [(ABPC + C)^{P}]/X$$

where:
- AR_{adj}: Adjusted Arrival Rate
- AR_{est}: Estimated Arrival Rate
- $ABPC$: Adjacent Blind Period Counter
- C, P, X: User Defined Constants

The longer the end of the queue stays "out of view", the higher the ABPC becomes and the more the adjusted arrival rate is increased in comparison to the estimated arrival rate. Extensive testing suggests that the following constants provide good predictive abilities, even during highly over-

saturated conditions where some vehicles experience as many as six phase failures: P = 0.4, C = 66, X = 30. These constants can be varied to change the shape of the predicted cumulative delay curve.

Non-Visible Queue Re-Adjustment Technique

As a queue becomes longer the back of the queue propagates closer to its source of arrivals. This tends to increase the effective arrival rate of vehicles at the end of the queue. Queue propagation becomes increasing important during over-saturated conditions as the volume-to-capacity ratio increases and extensive queues quickly form.

Figure 3 shows the result of our prediction process. The predicted non-visible delay is added to the measured visible delay to obtain the total predicted delay. The total predicted delay is reasonably close to the actual delay. The results are by no means perfect, but they are much better than the alternative, which is simply using the visible delay.

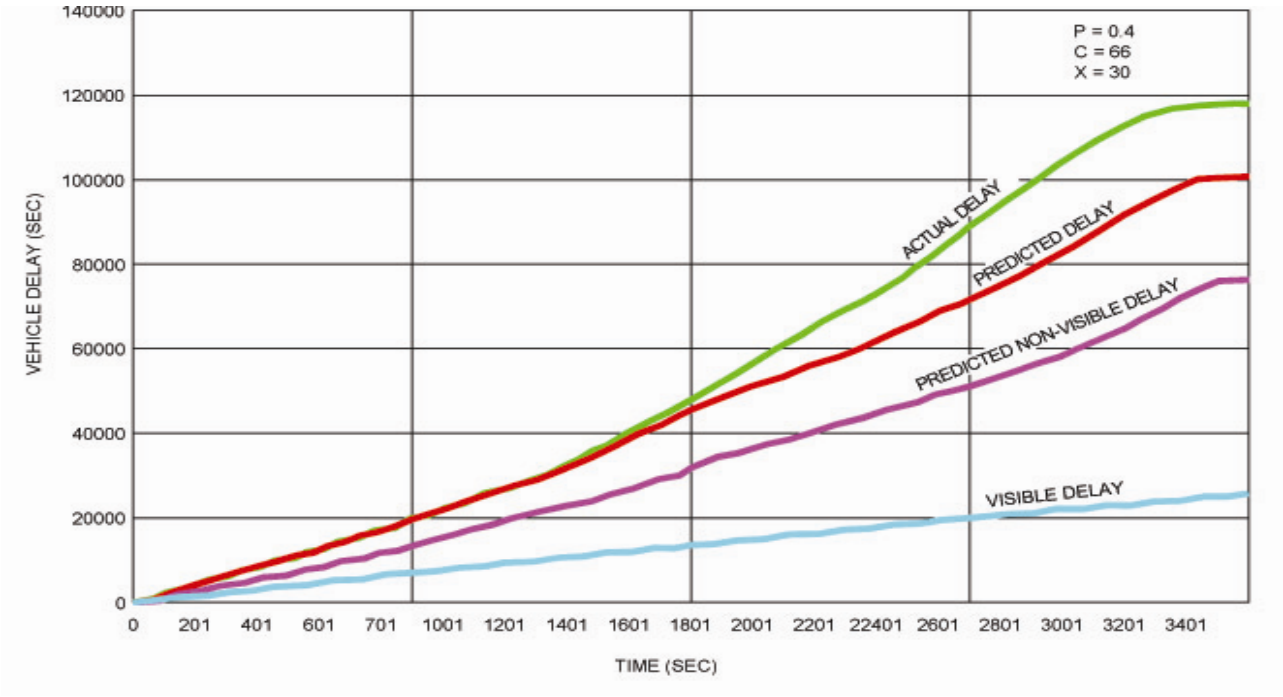

Figure 3. Cumulative stopped delay comparison

To demonstrate the prediction procedure, four examples based on a 120 second cycle length were developed. Each example uses a different set of arrival rates that result in over-capacity conditions at some point during the one-hour analysis time frame. Three CORSIM runs (replications) were made for each example with a different random number set used for each of the three replications.

Queue Prediction Results

A review of Figure 4 indicates that our prediction technique is fairly good at predicting back of queue position for all 12 runs, with the amount of error increasing somewhat as the v/c ratio increases. This is in stark contrast to the procedures contained in the Highway Capacity Manual

(and codified in the HCS+ software) which, as Figure 4 shows, grossly overestimates the back of queue position.

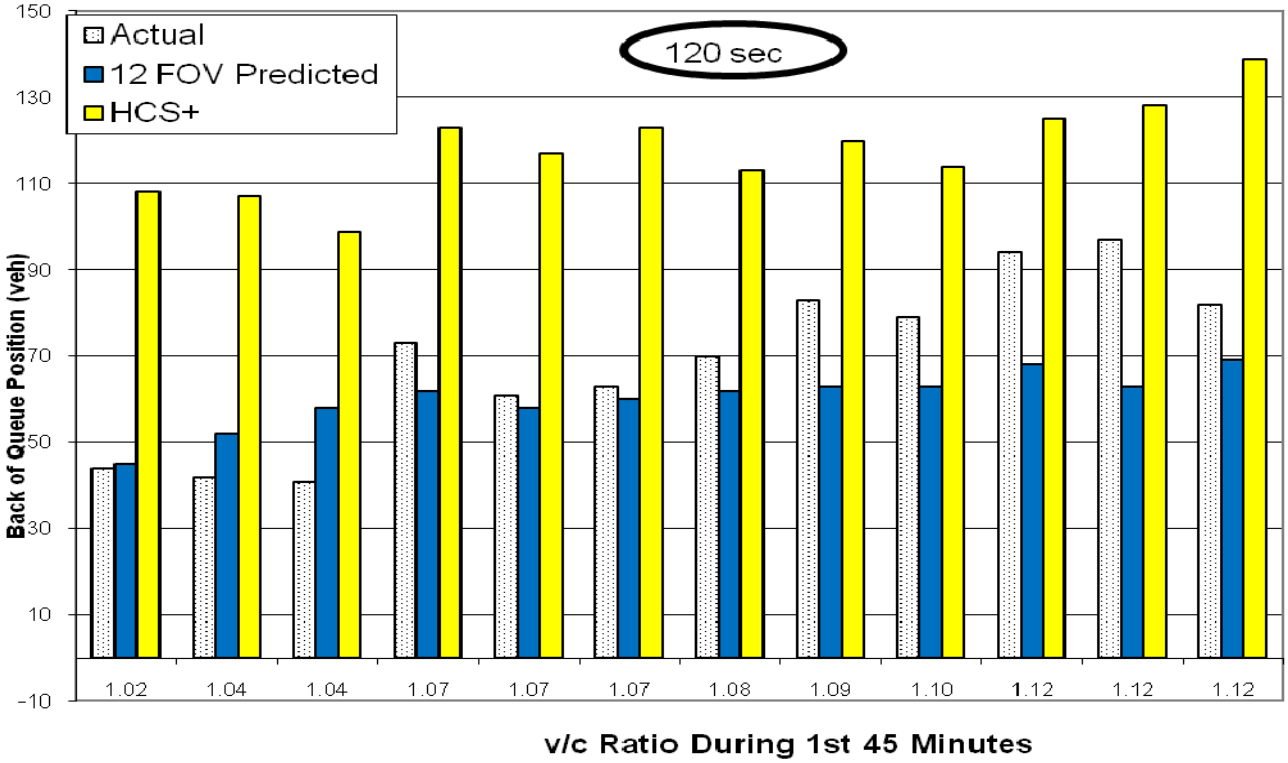

Figure 4. 98th percentile back of queue prediction

Figure 5 summarizes our stopped delay prediction results as compared to actual stopped delay. This figure indicates that our procedure also does a good job of predicting stopped delay over all v/c ratios.

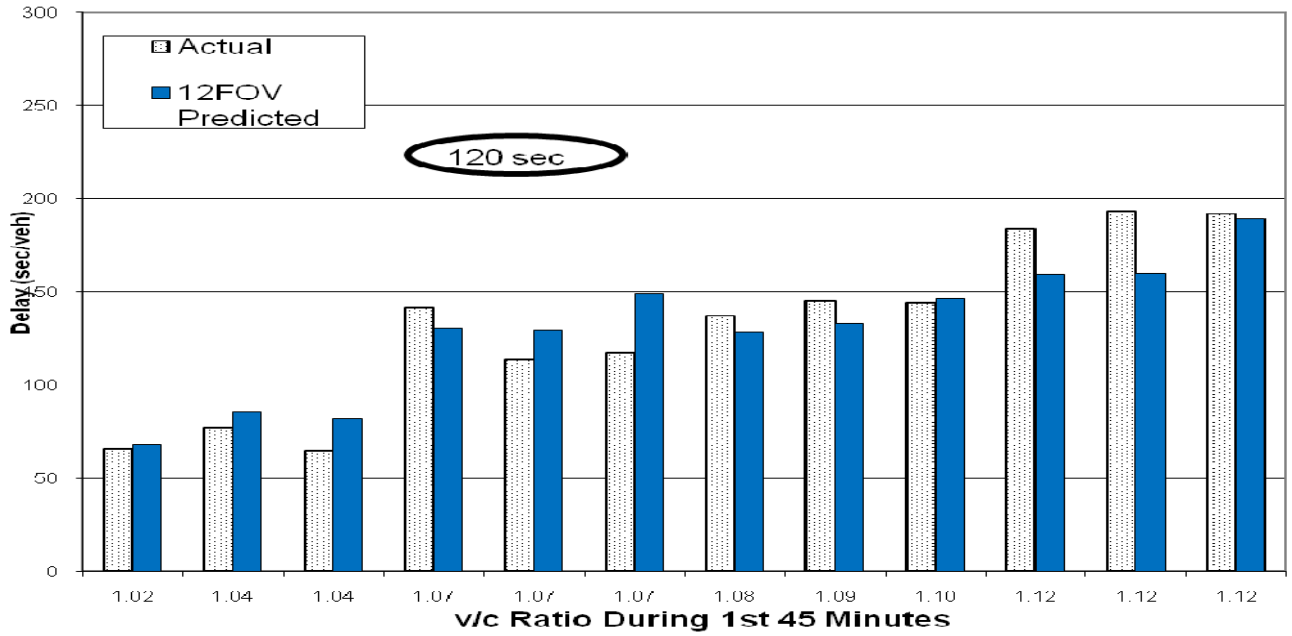

Figure 5. Stopped delay prediction

Figure 6 shows the relative contribution of each segment of our prediction methodology. For the examples under consideration, visible delay makes-up about 60% of total stopped delay when the v/c ratio is near 1.02 but only 20% of total stopped delay when the v/c ratio climbs to 1.12 This clearly demonstrates the need for this predictive procedure, at least for a rather typical case where the cycle length is 120 seconds and the field of view is limited to 12 vehicles. The first step in the predictive process uses an estimated arrival rate based on vehicles entering the field of view to predict the non-visible queue. This alteration increases the percentage of captured stopped delay to about 80% when the v/c is near 1.02 and to about 30% when the v/c is near 1.12. The results become reasonable for relatively low over-saturated v/c ratios but not for the higher ratios. The second step in the predictive process uses an adjusted arrival rate obtained from a power function adjustment that increases the estimated arrival rate based on the number of adjacent blind periods. This alteration increases the percentage of captured stopped delay to about 115% when the v/c is near 1.02 and to about 65% when the v/c is near 1.12. The results are still reasonable for relatively low over-saturated v/c ratios, and are greatly improved for the higher ratios, but the error for the higher ratios is still quite significant. The third step in the predictive process adjusts the non-visible queue length and associated delay due to queue propagation. This alteration has little or no affect on the percentage of captured stopped delay when the over-saturated v/c ratio is close to 1.0 but increases the percentage of captured stop delay to about 90% when the over-saturated v/c ratio is near 1.12. The results are now reasonable over all v/c ratios although a slight upward bias of about 15% exists at the lower over-saturated v/c ratios and a slight downward bias of about 10% exists at the higher v/c ratios. A tremendous improvement in stopped delay estimation is clearly provided by our procedure.

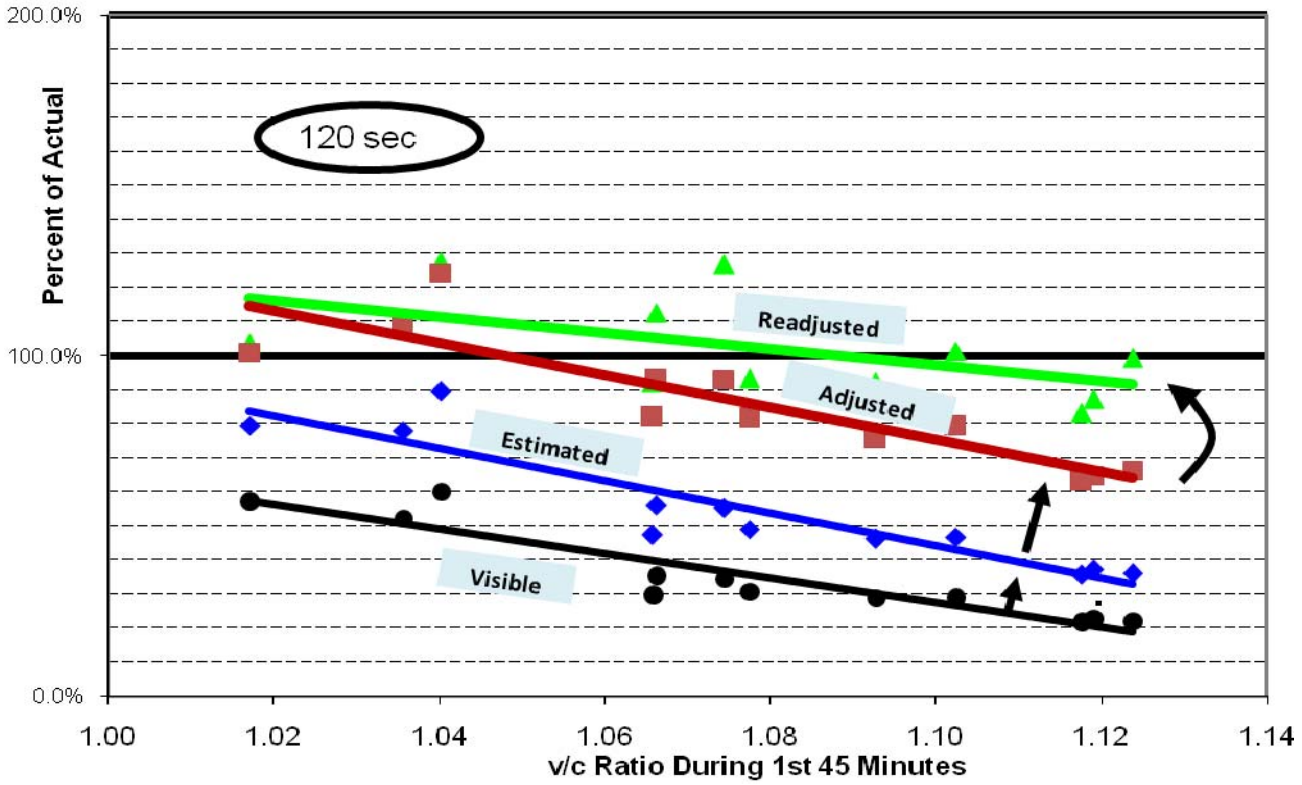

Figure 6. Stopped delay prediction

Figure 7 summarizes our control delay prediction results as compared to actual control delay. Our procedure does a reasonably good job of predicting control delay over all v/c ratios, even if we use a constant ratio of 1.3 to convert predicted stopped delay into predicted control delay. (Previous work has demonstrated that this factor actually varies by cycle length and v/c ratio.) Also included in Figure 7 is control delay as predicted by HCM procedures. The HCM procedures tend to over-predict control delay for the lower over-saturated v/c ratios.

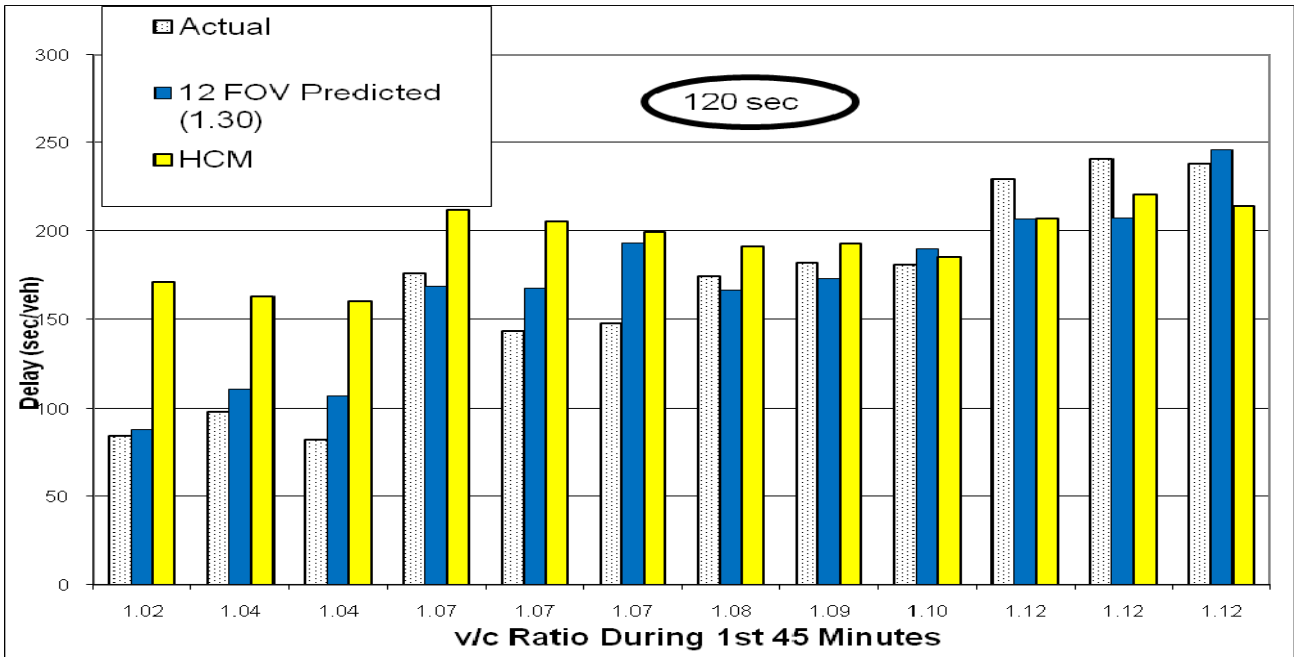

Figure 7. Control delay prediction

THEOREICAL BOUNDS FOR DELAY ESTIMATION

Our delay estimation procedure begins by calculating an estimated arrival rate. Then, if the back end of the queue is not visible, the procedure modifies the estimated arrival rate upward using a power function to predict the real arrival rate. This power function adjusts the rate in a manner that, in essence, varies with the amount of time during which the back end of the queue is not visible. A major advantage of this approach is that the resulting estimated queues and associated delay can be immediately calculated on a second-by-second basis, in real time. A major disadvantage of the approach is that there is no theoretical relationship between the departure rate and the real arrival rate. Under the right circumstances, errors can accumulate to the point that the delay estimation is no longer reasonable. The potential for this is highest when the length of time that the end of the queue is not visible covers most of the analysis time frame.

However, it is possible to calculate a set of theoretical upper and lower bounds on the solution space by using information obtained at the end of the analysis period when the arrival rate is known. In order to make any type of reasonable delay estimation, all queues must dissipate prior to the end of the analysis time frame. Once this occurs, a calculation of the arrival rate during the final portion of the analysis time frame, the last 15 minutes of the hour, can be made. Knowing this final arrival/departure rate and knowing the total number of vehicles that have crossed the stop bar during the entire hour we can, by assuming a reasonable minimum peak hour factor, work backwards

through the period to identify arrival curves that serve as both lower and upper bounds. These theoretical results can be used, in an ex post facto manner, to "bracket" the real-time delay estimation procedure presented in the previous chapter. An example of an upper bound cumulative arrival curve is provided as Figure 8 and an example of a lower bound cumulative arrival curve is provided as Figure 9.

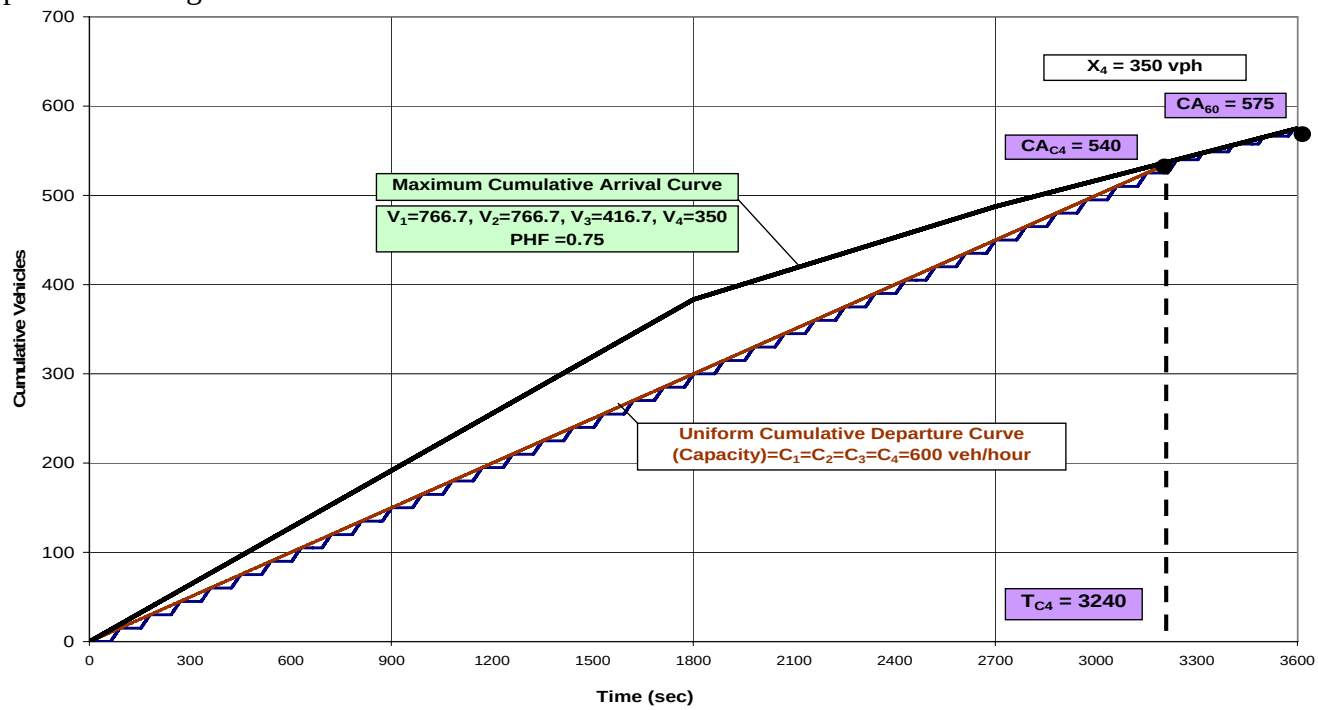

FIGURE 8. Maximum reasonable cumulative arrival curve

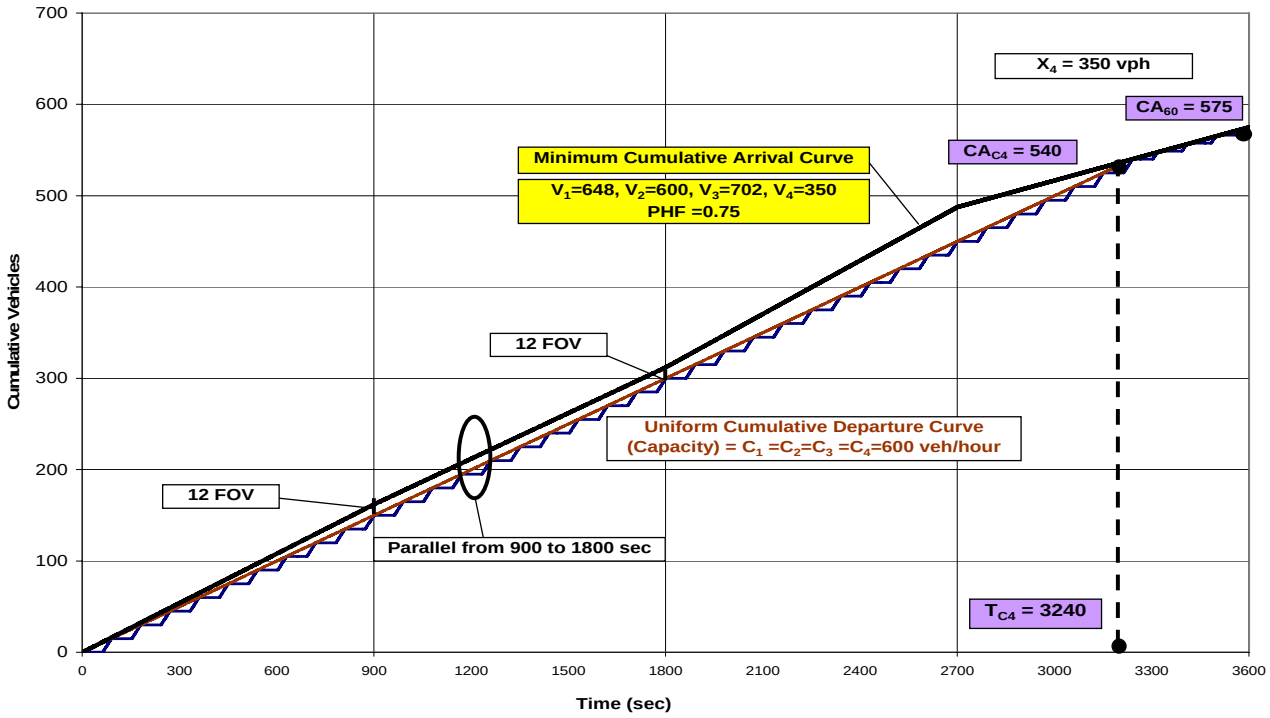

FIGURE 9. Minimum reasonable cumulative arrival curve

Unless the historical minimum peak hour factor is violated, the true cumulative arrival curve can be expected to lie somewhere between these two curves. Mathematical derivation of the formulas used to establish these curves is quite detailed and, for the sake of brevity, is not presented. It should be noted that formulas have been derived to predict the upper and lower bounds over any number of 15-minute periods, not just the four 15-minute period (one hour) example shown here. However, when more than four periods are examined the peak hour factor must be replaced by a generalized peak period factor.

Knowing the upper and lower bounds for the cumulative arrival curve we can calculate the associated maximum and minimum "cumulative curve delay", which is the area between the cumulative arrival curve and the cumulative departure curve. As is indicated Figure 10, cumulative curve delay is neither stopped delay nor control delay, but rather a composite measure that includes certain delay terms, excludes others, and includes other components of time that are not delay at all.

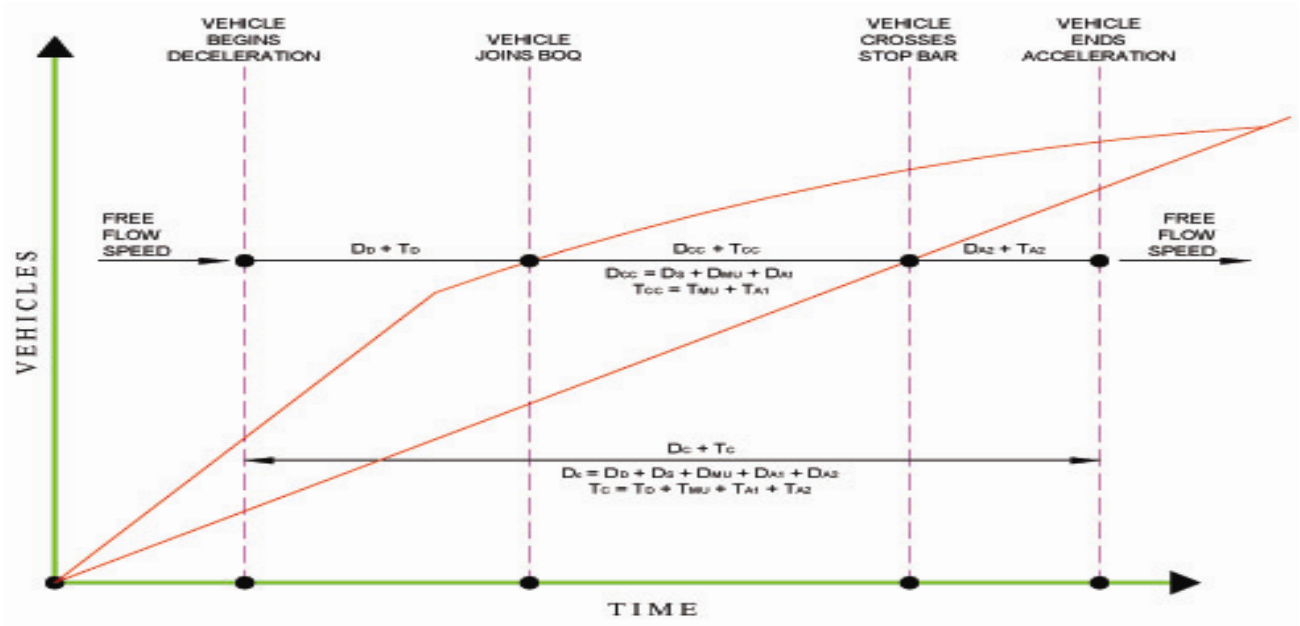

WHERE:

D_C	=	CONTROL DELAY
T_C	=	FREE SPEED TIME
D_D	=	DECELERATION DELAY
T_D	=	FREE SPEED DECELERATION TIME
D_{CC}	=	CUMULATIVE CURVE DELAY
T_{CC}	=	CUMULATIVE CURVE FREE SPEED TIME
D_S	=	STOPPED DELAY
D_{MU}	=	MOVE-UP DELAY
D_{A1}	=	PRE-STOP BAR ACCELERATION DELAY
D_{A2}	=	POST-STOP BAR ACCELERATION DELAY
T_{MU}	=	FREE SPEED MOVE-UP TIME
T_{A1}	=	PRE-STOP BAR FREE SPEED SPEED ACCELERATION TIME
T_{A2}	=	POST-STOP BAR FREE SPEED ACCELERATION TIME

FIGURE 10. Delay and Travel Time Components

Control delay is defined as the sum of deceleration delay, stopped delay, queue move-up delay, and acceleration delay. Cumulative curve delay includes the stopped delay and queue move-up delay but excludes deceleration delay and the portion of acceleration delay that occurs past the stop bar. It also includes two time components that are not delay at all, Free Speed Move-Up Time and Free Speed Acceleration Time Prior to the Stop Bar. Trajectory analysis indicates that, over a range of conditions, cumulative curve delay can be converted to stopped delay by applying a factor of about 0.75 Consequently, we must multiply the delay associated with the upper and lower bounds by this conversion factor before bracketing our prediction results. Table 1 provides the results for one of our example volume patterns.

Table 1. Average stopped delay prediction results for 700_725_625_350vph volume pattern

120 second cycle
Min PHF = 0.80

		Cumulative Stopped Delay			
Period:	0	1	2	3	4
S*g/L Capacity:		641	651	636	601
Arrivals at BOQ:		724	733	628	360
Actual PHF:		0.83			
Simulation Ground Truth	**0**	**13956**	**36458**	**67344**	**79196**
OD to D_S Conversion %		78%	76%	75%	76%
Actual		19711	56503	100266	117751
Corrected Actual	0	15374	43131	75534	89098
%Error		10.2%	18.3%	12.2%	**13%**
Maximum	0	22669	67791	116722	131985
Corrected Maximum	0	17681	51747	87930	99869
Minimum	0	11907	29826	58364	73610
Corrected Minimum	0	9288	22386	43967	55698
PHF Min %Error Predicted	0	12173	31246	58584	71450
%Error		-13%	-14%	-13%	**-10%**
BuckQ Predicted	0	15814	38171	62644	77988
%Error		13%	5%	-7%	**-2%**

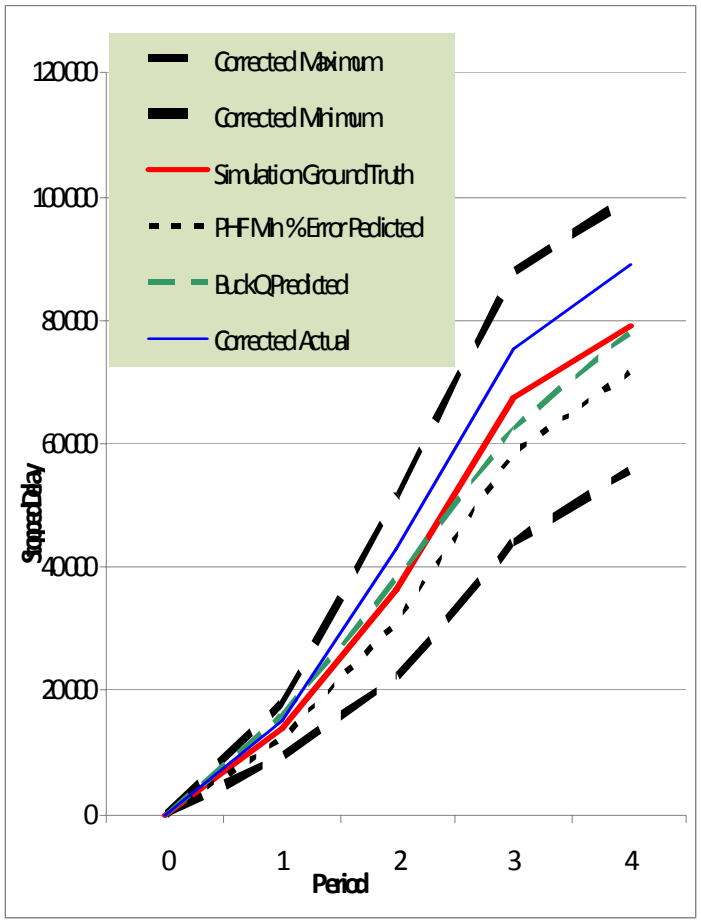

In this example, our prediction procedure produces a stopped delay after four 15-minute periods that differs from the true stopped delay by only 2%. As desired, the prediction curve stays below the upper bound (corrected maximum curve) and above the lower bound (corrected minimum curve) for the entire one hour analysis time frame.

Also provided in Table 1 is an independent estimate of the actual delay that is derived solely from the theoretical curves. This estimate minimizes the percentage errors when compared against both the minimum and maximum possible values using the following equation:

$$Y = 2UL/(U+L)$$

where: Y: Estimate that yields equivalent percentage errors
U: Upper Value (in this case the Maximum Delay)
L: Lower Value (in this case the Minimum Delay)

In the Table 1 example, this estimate differs from the true stopped delay by 10%.

CONCLUSIONS

A reasonably accurate real-time technique for estimating actual stopped delay under conditions of limited information was developed as a result of this research. The resulting procedure is capable of predicting the unseen component of delay for both under-saturated conditions and over-saturated conditions. The procedure utilizes a series of adjustments to the measured arrival rate entering the field of view to estimate the true arrival rate at the back of the queue. The primary rate adjustment is a function of the number of consecutive phase failures for the approach with a secondary adjustment made to account for queue propagation effects. The secondary adjustment increases in importance as the over-saturated volume-to-capacity ratio increases. Queue formation and dissipation associated with the predicted arrival rate is used to estimate total stopped delay, and conversion ratios based on volume-to-capacity ratio and cycle length are then used to derive control delay from stopped delay.

Under conditions of limited information, it is possible to calculate a set of theoretical upper and lower bounds on the solution space for approach delay by using information obtained at the end of the analysis period when all queues are visible and the arrival rate equals the departure rate. Knowing this arrival/departure rate and knowing the total number of vehicles that have crossed the stop line during the entire hour we can, by assuming a reasonable minimum peak hour factor, work backwards through the period to identify arrival curves that serve as both lower and upper bounds on delay. These theoretical bounds can be used, in an ex post facto manner, to bracket the real-time delay estimation procedure. They can also be used to identify an independent "most probable" arrival pattern by selecting an intermediate curve between the upper and lower bounds that minimizes the maximum percent error between the estimate and the actual delay**.**

REFERENCES

Tarnoff, P. and Ordonez, J. (2004), Signal Timing Practices and Procedures, Institute of Transportation Engineers, 1-3.

Highway Capacity Manual (2000), Transportation Research Board, National Research Council, Washington, D.C., 2000